A robust scheme for free surface and pressurized flows in channels with arbitrary cross-sections

ELISA ALDRIGHETTI, Ph. D. Student, Department of Mathematics, University of Trento, Via Sommarive 14, I-38050 Povo (Trento), Italy
GUUS STELLING, Full Professor, Fluid Mechanics Section, Faculty of Civil Engineering and Geosciences, Technical University of Delft, P.O. Box 5084,2600 GA Delft, The Netherlands.

SUMMARY

Flows in closed channels, such as rain storm sewers, often contain transitions from free surface flows to pressurized flows, or vice versa. These phenomena usually require two different sets of equations to model the two different flow regimes. Actually, a few specifications for the geometry of the channel and for the discretization choices can be sufficient to model closed channel flows using only the open channel flow equations. Transitions can also occur in open channels, like those from super- to subcritical flow, or vice versa. These particular flows are usually difficult to reproduce numerically and strong restrictions are imposed on the numerical scheme to simulate them. In this paper, an implicit finite-difference conservative algorithm is proposed to deal properly with these problems. In addition, a special flux limiter is described and implemented to allow accurate flow simulations near hydraulic structures such as weirs. A few computational examples are given to illustrate the properties of the scheme and the numerical solutions are compared with experimental data, when possible.

KEY WORDS: Saint Venant equations; free surface flow; pressurized flow; supercritical flow; subcritical flow; transitions; hydraulic jumps; flux limiter

1 Introduction

The transition from free surface to pressurized flow or vice versa is a phenomenon often occurring in closed channels.

This situation may happen for example in storm sewers systems during heavy storm events or even in a closed channel with initially free surface flow as a result of the start-up of machinery (turbines, pumps, gates).

Because of the wide range of practical problems involving closed channel flows, numerical methods are needed to predict the water profile, pressure and discharge during pipes pressurization and depressurization.

The one-dimensional equations for free surface as well as pressurized flows in closed channels are essentially the Saint Venant Equations:

$$A_t + Q_x = 0 \tag{1}$$

$$Q_t + (UQ)_x + gA\eta_x + c_f \frac{|U|}{R_H} Q = 0 \tag{2}$$

where U is the cross-sectional averaged water velocity, η is the water level for free surface flows and the pressure head for pressurized flows measured vertically from a reference datum, $A(x, \eta(x,t))$ is an arbitrary but prescribed function of space and water surface elevation representing the cross-section area and $Q = AU$ is the discharge; g is the gravitational constant, c_f is a non-negative friction coefficient (see, e.g., Reference [3] for the definition) and R_H is the hydraulic radius.

Moreover, $H = \eta + h$, where H is the total water depth and h is the depth below reference plane.

Two types of algorithms broadly used in the literature for the numerical solution of the Saint Venant Equations are the explicit and the implicit ones.

Explicit algorithms are such that the time step is limited to the Courant condition. This limitation cannot be fulfilled for pressurized flows due to the infinite propagation velocities. In fact, assuming the incompressibility of water, the wave celerity is infinite in pressurized sections and the same explicit algorithm used for the free surface flow part of the domain cannot be used to solve the pressurized parts.

To avoid this inconvenience, almost all existing models use the Preissmann slot technique [4, 5, 8], that is an approximation of the real, closed section with an open section displaying a very small top width, called Preissmann slot.

In case of free surface flows the slot has no effects and the open channel flow Equations apply as usual.

Moreover, in case of pressurized flows, the small slot allows a finite value of the wave celerity and the use of the free surface flow model everywhere in the computational domain.

A delicate issue is the choice of the slot width ϵ. In fact, if ϵ is too small, the use of the Preissmann approximation can produce a large wave celerity and a corresponding strict time step limitation, while, if ϵ is too large, inaccuracies may results.

On the other hand, unconditionally stable methods like fully implicit methods [2, 10] are able to simulate the transition from free surface to pressurized flow in channels with closed sections without any approximation of the section geometry. In fact, assuming the incompressibility of water, they can manage instantaneous transmission of pressure and velocity changes arising in the pressurized part of the channel.

In the present paper, the performance of the numerical scheme presented in Reference [1] is investigated for the simulation of free surface as well as pressurized flows in closed channels. This technique is semi-implicit in time, fully water volume conservative, satisfies a correct momentum balance near large gradients and deals properly with problems presenting flooding and drying. For the reasons mentioned above, in case of closed channel flow the fully implicit version of this technique will be considered here.

This paper is organized in 5 sections. In Section 2 a brief description of the numerical scheme for the discretization of the Equations (1) and (2) is given. A special flux limiter function is described in Section 3 to face the problem of low resolution in case of critical flows. Section 4 presents a test to verify its behaviour and shows the ability of the scheme in dealing with weir flows, for both critical and subcritical situations including the transition. The first part of Section 5 presents the numerical results obtained solving the pressurization of a horizontal pipe and shows the comparison with the experimental data used by Wiggert in Reference [11]. Finally, the numerical scheme is validated simulating a flow in a horizontal and downwardly inclined pipe and comparing the numerical results with the experimental data obtained in the laboratory.

2 Numerical method

Equations (1) and (2) are discretized in the spatial interval [0,L] on a space staggered grid whose nodes are denoted by x_i and $x_{i+1/2}$, $i = 0, N+1$. The discrete discharge $Q_{i+1/2}$ (or the velocity $U_{i+1/2}$) is defined at half integer nodes and the discrete variable η_i, representing the water level for free surface flows and the pressure head for pressurized flows, is defined at integer nodes as well as the cross-sectional area A_i and the bottom h_i.

An implicit discretization in time is chosen in order to obtain an efficient and stable numerical method able to cope with free surface flows as well as with pressurized flows.

Specifically, the continuity Equation (1) is inte-

grated in time to obtain

$$V_i(\eta_i^{n+1}) = V_i(\eta_i^n) - \Delta t\theta[Q_{i+1/2}^{n+\theta} - Q_{i-1/2}^{n+\theta}] \quad (3)$$

where $V_i(\eta_i) = \int_{x_{i-1/2}}^{x_{i+1/2}} A dx$ is, in general, a non linear function of η representing the volume occupied by the water [1] and $Q^{n+\theta} = \theta Q^{n+1} + (1-\theta)Q^n$.

Moreover, the scheme for the momentum Equation (2) is the following

$$(1 + c_f \frac{|U|_{i+1/2}^n}{R_H}\Delta t)Q_{i+1/2}^{n+1} + \\ + gA_{i+1/2}^n \theta \frac{\Delta t}{\Delta x_{i+1/2}}(\eta_{i+1}^{n+\theta} - \eta_i^{n+\theta}) = F_{i+1/2}^n \quad (4)$$

where $F_{i+1/2}^n$ is a finite difference operator including the explicit discretizations of the advective and the free surface (or pressure head) slope terms [1].

From the point of view of the spatial discretization, the discharge is defined as $Q_{i+1/2} = A_{i+1/2}U_{i+1/2}$.

Therefore, remembering that the cross sectional area A, the variable η and the bottom h are initially defined at integers nodes, it is necessary to define explicitly their value at the half integer node $i + 1/2$.

To do this, the following upwind rule based on the sign of the momentum $Q_{i+1/2}$ is used for the definition of η

$$\eta_{i+1/2} = \begin{cases} \eta_i & \text{if} \quad Q_{i+1/2} \geq 0 \\ \eta_{i+1} & \text{if} \quad Q_{i+1/2} < 0 \end{cases}, \quad (5)$$

while the value of the bottom $h_{i+1/2}$ is given by

$$h_{i+1/2} = max(h_i, h_{i+1}), \quad (6)$$

except for the case we can analytically express it as $h_{i+1/2} = h(x_{i+1/2})$.

3 A flux limiter for critical flows

A special flux limiter function has been constructed to be used in the extrapolation of the value $\eta_{i+1/2}$ in case of critical flows and it is given, assuming positive flow direction, by the following relation

$$\Psi_{i+1/2} = \Psi(x_{i+1/2}) = min(0, max(\frac{-\eta_i/3}{\eta_{i+1} - \eta_i}, 1)) \quad (7)$$

One can show that

$$0 \leq \Psi_{i+1/2} \leq 1$$

that means that a data reconstruction using the flux limiter function Ψ defined in (7) is consistent, because it is a Total Variation Non Increasing (TVNI) scheme, as stated in the Harten's Theorem [6].

In particular, the reconstruction of η in the node $i + 1/2$ assumes the following form for $x \in [x_{i-1/2}, x_{i+1/2}]$

$$\eta(x) = \eta_i + \frac{(x - x_i)}{\Delta x}\Psi(x)(\eta_{i+1} - \eta_i) \quad (8)$$

and can be written in a more compact notation as follows

$$\eta_{i+1/2} = min(\eta_i, max(\frac{2}{3}\eta_i, \eta_{i+1})). \quad (9)$$

The derivation of this special flux limiter follows from the analysis of the specific energy head function [3] in case of a constant discharge

$$E = H + \frac{U^2}{2g}. \quad (10)$$

This function assumes its minimum respect to H in the case of critical flows, that is if $Fr = 1$ ($U = \sqrt{gH}$), and its minimum value is

$$E = \frac{3}{2}(\frac{Q^2}{gA^2})^{\frac{1}{3}} \quad (11)$$

where $H_{cr} = (\frac{U^2}{g})^{\frac{1}{3}}$ is called critical depth.

Thus, in case of critical flow, one has $H = \frac{2}{3}E$ (see, e.g., [3]).

Equation (9) is finally obtained assuming that the squared velocity is negligible with respect to H and introducing a min-max rule to ensure consistency.

The implementation of this flux limiter improves the accuracy of the method and helps in facing the problems arising in case of low resolution of the grid. An application of this flux limiter can be found in Section 4.

4 Open channels tests

The first test presented in this section simulates a steady state problem including a hydraulic jump over a non-flat bed profile in a rectangular frictionless channel.

A hydraulic jump consists in the transition from a supercritical flow to a subcritical flow, it is extremely turbulent and characterized by a strong energy dissipation.

In the analysis of supercritical flows, the main aspect to be investigated is the location of the hydraulic jump.

On the other hand, in case of subcritical flows, a precise estimation of the energy head loss due to the hydraulic jump is essential to have the correct upwind water level and the correct discharge over the sill once the downstream water level is fixed.

The numerical test presented in this section shows the ability of the numerical method and of the flux limiter function provided by (9) in fulfilling these requirements, even in the case of a low resolution grid.

The domain length is $L = 100m$ and in the middle of the channel there is a sill with a crest of $1m$ height and $10m$ long and the tangent of the slopes of the sill are abrupt within one grid cell.

Moreover, there are two open boundaries, the inflow and the outflow, where a discharge of $1m^3/s$ and a water depth of $1m$, respectively, are imposed [9].

The discretization parameters are $c_f = 0$, $g = 9.81m/s^2$, $\theta = 1$ and $\Delta t = 10^{-3}s$.

Figure 1 shows a comparison between the numerical solutions obtained for 100 grid points using the flux limiter (7) only over the sill (*Solution 1*) and the numerical solutions obtained for 20 grid points with (*Solution 2*) and without (*Solution 3*) the help of the flux limiter.

The numerical *Solutions* 1 and 2 are coincident in almost all the nodes in common (and in particular at the upstream end) altough the second grid is five times coarser than the first.

Moreover, on equal grid size, the numerical solution obtained using the limiter (*Solution 2*) shows an upstream water level that is consistent with that of *Solution 1* and higher than that obtained without the limiter (*Solution 3*): the reduction of the resolution of the grid causes the upstream water level to decrease in

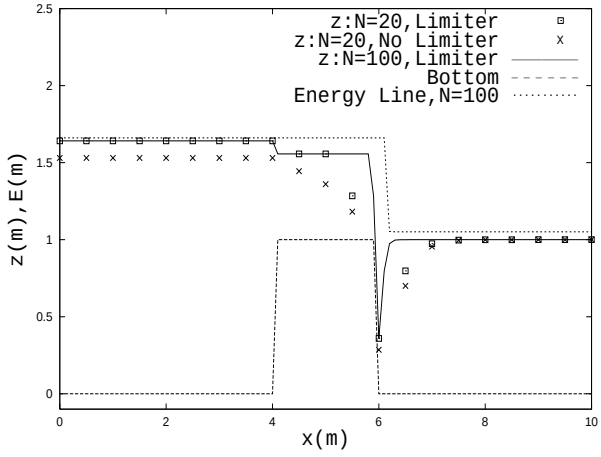

Figure 1: High and low resolution grids: effect of the flux limiter

the numerical solution of the first order model.

The quality of the results can also be appreciated from the approximation of the energy line plotted in Figure 1: as one can see, it is constant everywhere, except near the hydraulic jump where the energy head drops as is to be expected by considerations based on open channel hydraulics [3].

The second test presented in this section is an interesting proof of the robustness of the proposed scheme in simulating continuous transitions from subcritical to supercritical flow and vice versa.

These transitions are obtained imposing as downstream boundary condition a water level following the hydrograph depicted in Figure 2 and described by the equation

$$\eta(L,t) = 0.8sin(0.01t) + 1 \tag{12}$$

Figure 3 shows the numerical results obtained for the upstream water level during two complete oscillations of the downstream boundary condition (12).

As expected, in the range for $\eta(L,\cdot)$ corresponding to imperfect weirs, any small change of its value affects the upstream flow condition, because the wave celerity is larger than the flow velocity.

On the other hand, in the range for $\eta(L,\cdot)$ corresponding to perfect weirs, a downstream disturbance

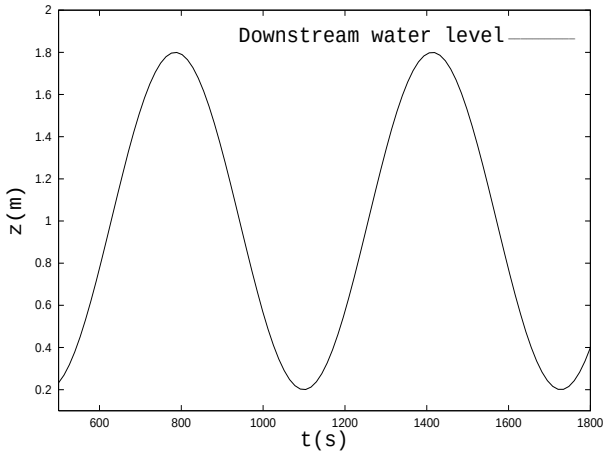

Figure 2: Downstream boundary condition on the water level

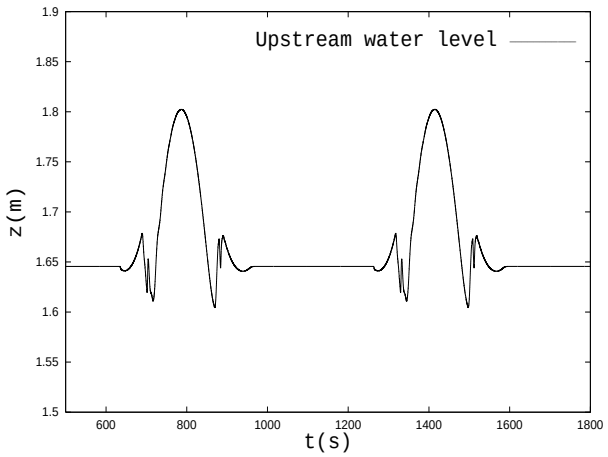

Figure 3: Upstream water level: effects of varying downstream boundary condition

does not travel upstream and identical upstream depth estimations are produced.

5 Closed channel tests

In this section, the numerical results obtained by the algorithm presented in Reference [1] modelling a flow in a horizontal and in a horizontal and downwardly inclined pipe are compared with the experimental data.

Before presenting these test problems, a few specifications regarding the geometrical and the physical quantities involved in them are needed.

In case of free surface flows in a closed channel, as well as for open channel flows, η is the instantaneous water surface elevation measured vertically from a reference datum and assuming an horizontal interface between water and air, the quantities H and A have the usual definitions.

In case of pressurized flows, η plays the role of the pressure head, the water height H is the maximum height reachable $H_{top} = \eta_{top} + h$ and the wetted area A is the area of the whole cross section A_{top}.

Therefore, the total water depth H in a closed channel can be expressed as follows

$$H = \begin{cases} \eta + h & \text{if} \quad \eta \leq \eta_{top} \\ H_{top} & \text{if} \quad \eta > \eta_{top}. \end{cases} \tag{13}$$

Moreover, the cross-sectional area A in a closed channel is a piecewise derivable non decreasing functions of η and it is defined depending on the channel geometry.

For a rectangular closed channel with constant width B one has $A = BH$, while for the special case of a circular channel with diameter D it holds

$$A = \begin{cases} \frac{D^2}{4}\left[arccos(1-\frac{2H}{D}) - (1-\frac{2H}{D})\sqrt{1-(1-\frac{2H}{D})^2}\right] & \\ \qquad\qquad\qquad\qquad \text{if} \quad \eta \leq \eta_{top} & \\ \pi(D/2)^2 \qquad\qquad\qquad \text{if} \quad \eta > \eta_{top} & \end{cases} \tag{14}$$

5.1 Pressurization in a rectangular pipe

This test [5] reproduces a free surface and pressurized flow in a horizontal, rough, rectangular, closed channel

of length $L = 10m$, width $B = 0.51m$, height $H_{top} = 0.148m$ and $c_f = g\frac{n_M^2}{R_H^{1/3}}$, where $n_M = 0.12$ is the Manning's roughness coefficient [3].

The upstream boundary condition is the hydrograph for the pressure head described in Figure 4, while the downstream boundary condition is a fixed water level, $H_{N+1} = 0.128m$.

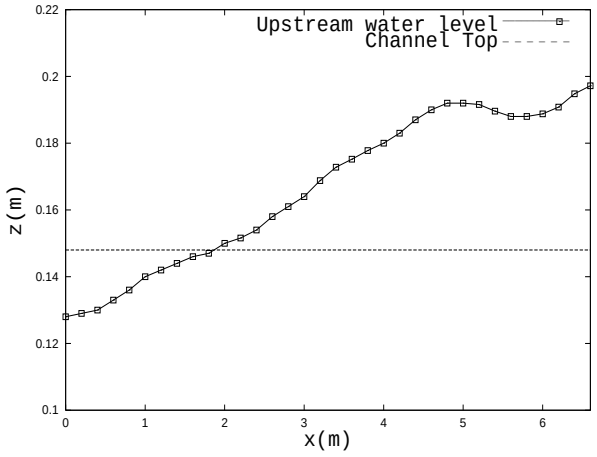

Figure 4: Water height at the upstream boundary against time.

Initially the following free surface flow conditions with still water are present:

$$U(x,0) = 0m/s, \quad \eta(x,0) = top(x) = 0.128 \qquad (15)$$

Then a wave, coming from the outside left side, causes the closed channel to pressurize starting from upstream. The interface separating pressurized from free surface flow moves from upstream to downstream as a front wave.

The physical and computational parameters are $g = 9.81m/s^2$, $\Delta x = 0.1m$, $\theta = 1.$ and $\Delta t = 5.\ 10^{-3}s$.

Figure 5 shows the behaviour of the numerical instantaneous pressure head η against time at $x = 3.5m$ compared with the experimental data [5]. The agreement is satisfactory.

5.2 Hydraulic jump in a circular pipe

These experiments have been carried out by the University of Delft and Delft Hydraulics in collaboration with the majority water boards in the Netherlands [7].

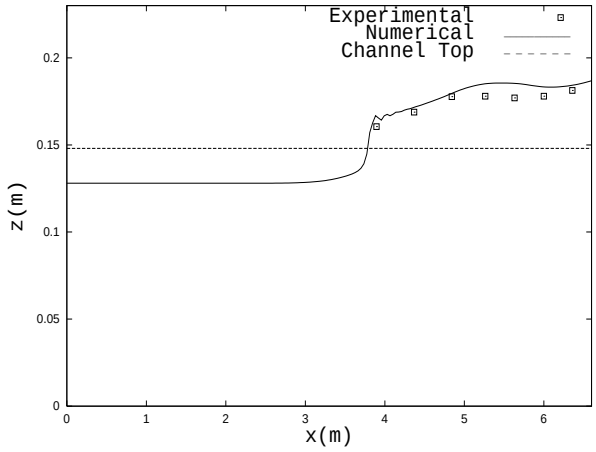

Figure 5: η at $x = 3.5$ against the time.

The aim of these experiments is the investigation about the air-water phenomena in wastewater pressure mains with respect to transportation and dynamic hydraulic behaviour. Free gas in pressurized pipelines can in fact significantly reduce the flow capacity and may cause undesirable efficiency loss.

These experiments have been conducted in a dedicated facility for research on gas pockets that are located at the transition from horizontal to inclined pipes.

The test section of the pipe consists of three parts: a horizontal pipe of length $L_1 = 2m$, a downward inclined pipe ($\alpha = 10°$) of length $L_2 = 4m$ and a horizontal pipe of length $L_3 = 2m$. The pipes have an inner diameter of $220mm$ and are made of transparent material (Perspex with equivalent sand roughness height of $k_s = 0$).

Injecting air into the water and preserving a constant water discharge at the inlet of the pipe and a constant pressure head downstream, an air pocket appears in the inclined part of the pipe and the obtained configuration presents similarities with hydraulic jumps in open channels.

The numerical results of the present model for the pressure head at the steady state of the phenomenon are compared with the experimental data. They are given as measurements of the water depth in a certain number of nodes located along the air pocket at a distance of about $30cm$ one to the other. The hydraulic jump is located

after at most $30cm$ from the last measurement.

Table 1 summarizes the boundary conditions imposed on the scheme in performing different tests.

Test	1	2	3	4
$Q_{1/2}$ (l/s)	30	36	40	45
η (m)	0.554	0.583	0.634	0.69

Table 1: Boundary Conditions

The physical and computational parameters are $g = 9.81m/s^2$, $\Delta x = 0.06m$, $\theta = 1.$ and $\Delta t = 10^{-2}s$.

Figures 6, 7, 8, 9 show a good agreement between the measured and the predicted data.

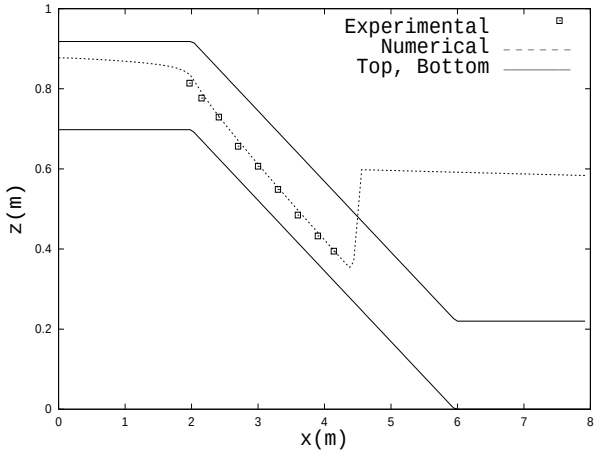

Figure 6: Test 1.

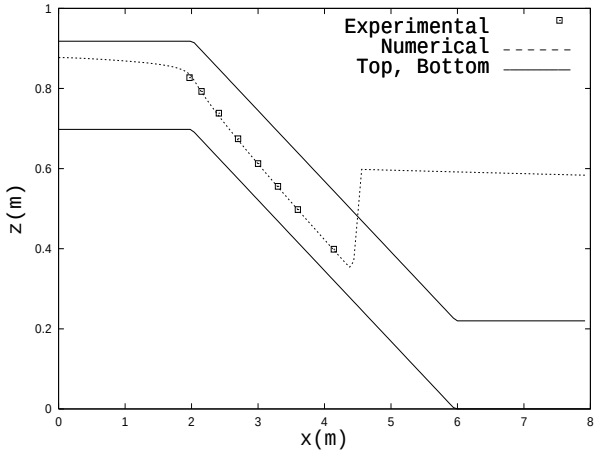

Figure 7: Test 2.

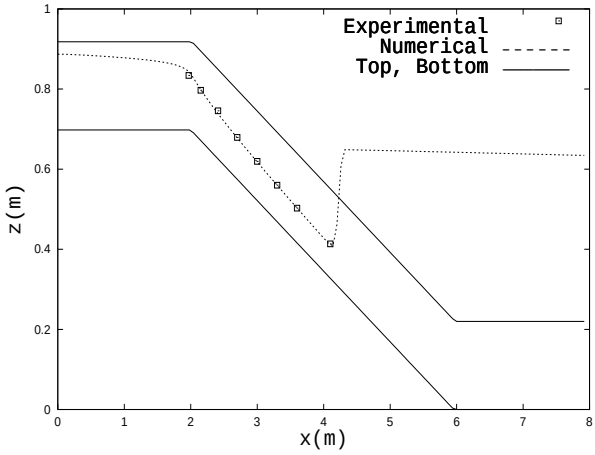

Figure 8: Test 3.

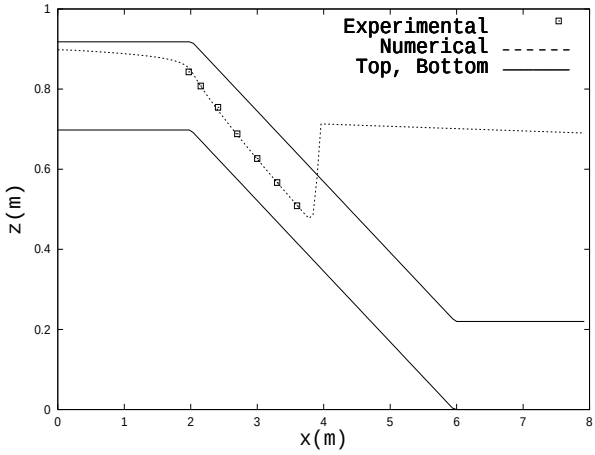

Figure 9: Test 4.

6 Conclusions

The performance of the one dimensional, conservative, semi-implicit finite difference model presented in Reference [1] in simulating free surface as well as pressurized flows in channels with arbitrary cross-sections has been investigated. A special flux limiter has been described and implemented to allow accurate flow simulations near hydraulic structures such as weirs, for both critical and subcritical situations including the transition. Some numerical test has been carried out in order to show the performance of the model. The numerical results have been validated against the experimental data, when possible.

List of symbols

Q = water discharge
U = water velocity
η = water level or pressure head (z in Figures)
H = total water depth ($H = \eta + h$)
$-h$ = bottom of the channel
A = cross-section area
V = volume
L = channel length
B = channel width
D = diameter
g = gravitational constant
c_f = friction coefficient
n_M = Manning coefficient
R_H = hydraulic radius
k_S = equivalent sand roughness height
N = number of nodes of the spatial grid
x = space
t = time
Δx = spatial grid size
Δt = time step
θ = parameter for the discretization in time
α = inclination
ϵ = Preissmann slot width
Ψ= flux limiter function
E = energy head
top = top level value in a closed conduit
i = element index
n = time level index
cr = value corresponding to critical flows

References

[1] Aldrighetti E, Zanolli P. A high resolution scheme for flows in open channels with arbitrary cross-section. *International Journal for Numerical Methods in Fluids.* 2005; **47**:817-824.

[2] Casulli V, Cattani E. Stability, accuracy and efficiency of a semi-implicit method for three dimensional shallow water flows. *Computers & Mathematics with Application.* 1994; **15**(6):629-648.

[3] Chanson H. *The Hydraulics of Open Channel Flow: An Introduction.* 1999; John Wiley & Sons Ltd.

[4] Cunge J.A, Holly F.M, Verwey A. *Practical Aspects of computational river hydraulics.* Pitman Publishing, 1980.

[5] Garcia-Navarro P, Priestley A. An implicit method for water flow modelling in channels and pipes. . *Journal of Hydraulic Research.* 1994; **32**: 721-742.

[6] Harten A. High resolution schemes for hyperbolic conservation laws. *Journal of Computational Physics.* 1983; **49**: 357-393.

[7] Lubbers CL, Clemens F.H.L.R. Capacity reduction caused by air intake at wastewater pumping stations. (Experiments of transport of gas in pressurized wastewater mains.) Technical Report, Section of Sanitary Engineering, Faculty of Civil Engineering and Geosciences, Delft University of Technology, The Netherlands, 2005.

[8] Sjoberg A. Calculation of Unsteady Flows in regulated rivers and Storm Sewer System Division

of Hydraulics, Chalmers Univ. of Technology, Goteborg, Sweden, 1976.

[9] Stelling GS, Duinmeijer SPA. A staggered conservative scheme for every Froude number in rapidly varied shallow water flows. *International Journal for Numerical Methods in Fluids.* 2003; **43**:1329-1354.

[10] Tucciarelli T. A new algorithm for a robust solution of the fully dynamic Saint-Venant Equations. *Journal of Hydraulic Research.* 2003; **3**:239-243.

[11] Wiggert DC and Sundquist MJ. Fixed grid characteristics for pipeline transients. *Journal of hydraulic division.* 1978; **103**:1403–1415.